

# Modeling Of A Solar Pond For Different Insulation Materials To Calculate Temperature Distribution

**Ismail Bozkurt**

Department of Mechanical Engineering, Faculty of Engineering, University of Adiyaman, Adiyaman 02040, Turkey  
ibozkurt@adiyaman.edu.tr

**Haci Sogukpinar**

Department of Energy Systems Engineering, Faculty of Technology, University of Adiyaman, Adiyaman 02040, Turkey  
hsogukpinar@adiyaman.edu.tr

**Mehmet Karakilcik**

Department of Physics, Faculty of Arts and Sciences, University of Cukurova, Adana 01330, Turkey

**Abstract**—Solar energy is an important source to meet energy demands. Therefore, investigations on solar energy systems are progressing rapidly. One of the solar energy systems is solar pond. Solar pond consists of three different zones such as Heat Storage Zone (HSZ), Non-Convective Zone (NCZ) and Upper Convective Zone (UCZ). These zones' density increases with depth. This structure prevents heat loss by convection in the inner of the solar pond. In the study, numerical simulation of a solar pond was conducted to determine the temperature distribution for different insulation materials (e.g. glass wool, foam and rock wool). As a result, it is observed that foam is better insulating materials with respect to two other insulating materials.

**Keywords**— Solar energy, solar pond, modeling, temperature distribution

## I. INTRODUCTION

Turkey has high solar energy potential because of its location in the northern hemisphere. Therefore, it is of worth to investigate and conduct research on this solar energy source [1]. With big resources and cost improvements, solar energy can clearly play a significant role in the energy demands. There are many systems to produce energy from the sun. One of these systems is solar pond. Solar ponds are constructed by using different salt (e.g. sodium chloride, magnesium chloride, calcium chloride). Solar pond consists of salty water layers with increasing density toward the bottom of the pond. This density difference prevents convection heat losses in solar pond. Thus, a large part of the incident solar energy can be stored in the storage zone.

Recent years, many studies have been done to investigate the performance of solar pond. Karakilcik et. al. [2] investigated the temperature distributions in an insulated solar pond, particularly during day-times and night-times. The total heat losses from the inner surface of the pond and its bottom and side walls, as a function of temperature difference were determined. Sakhrieh and Al-Salaymeh [3] studied both experimental and numerical parts of solar pond performance under Jordanian climate conditions. The

maximum temperature was determined at 47 °C in the heat storage zone in spring time. Karakilcik et. al. [4] presented an experimental investigation of energy distribution, energy efficiency and ratios of the energy efficiency with respect to shading effect on each zones of a small rectangular solar pond. Dah et. al. [5] evaluated the temperature and salinity profiles in a salinity gradient solar pond by using a small model pond. The maximum temperature attained in the storage zone was 45 °C carrying out a difference in temperature between the bottom and the surface of the pond. Bozkurt and Karakilcik [6] investigated the effect of the sunny area ratios on thermal efficiency of model solar pond for different cases. Solar ponds were modeled to compute theoretical sunny area ratios of the zones and temperature distributions in order to find the performance of the model solar ponds.

The thermal insulation is very important to increase the performance of the solar pond. In this study, we investigated numerical simulation of a solar pond to determine the temperature distribution for different insulation materials (e.g. glass wool, foam, rock wool).

## II. SOLAR POND

Solar pond is composed of zones with different density salty waters. These zones are Heat Storage Zone (HSZ), Non-Convective Zone (NCZ) and Upper Convective Zone (UCZ). The density of the solar pond increases through to the bottom of the solar pond. UCZ is filled with fresh water. NCZ acts as an insulating layer of the pond. The density in NCZ increases with increasing depth of the gradient layers. HSZ is formed by high density salty water which absorbs the solar radiation and stores [7]. Figure 1 shows computational domain and boundary condition for the model solar pond system. In the model, the thicknesses of HSZ, NCZ and UCZ are assumed as 0.90 m, 0.50 m and 0.10 m, respectively. The ranges of the salt gradient in the inner zones are 1000 kg/m<sup>3</sup> in UCZ, 1030-1150 kg/m<sup>3</sup> in NCZ and 1180 kg/m<sup>3</sup> in HSZ. The solar pond was designed as a rectangular prism with using steel. The insulation of the solar pond was made with different materials with 10 cm thickness.

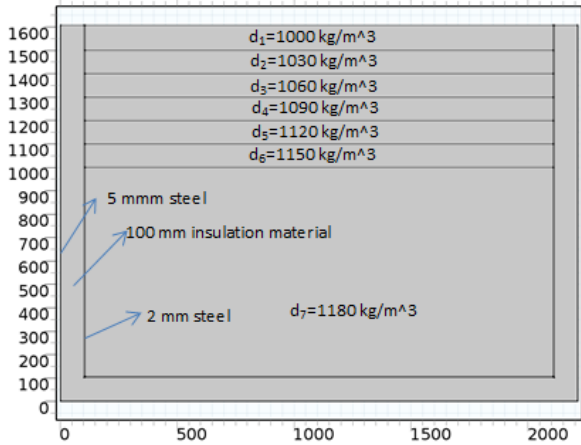


Figure 1. Computational domain and boundary condition

### III. MODELLING OF THE SYSTEM

In this study, "Radiation in Participating Media (rpm)" user interface was used to calculate temperature distribution in the solar pond. This interface solves for radiation intensity field. The Radiation in Participating Media node uses the radiation transfer equation that is expressed with equation (1):

$$\Omega \cdot \nabla I(\Omega) = \kappa I_b(T) - \beta I(\Omega) + \frac{\sigma_s}{4\pi} \int_0^4 I(\Omega') \phi(\Omega', \Omega) d\Omega' \quad (1)$$

Where,  $I(\Omega)$  is radiation intensity,  $T$  is temperature,  $\kappa, \beta, \sigma_s$  are absorption, extinction and scattering coefficient respectively,  $I_b$  is blackbody radiation intensity and  $\phi$  is the scattering phase function.

The balance of the radiation intensity includes all contributions and they are propagation, emission, absorption, and scattering. In order to pair radiation in participating media, radiation heat flux must be taken into account intercalary and conductive heat flux and heat transfer equation in terms of temperature becomes (2),

$$\rho C_p \left( \frac{\partial T}{\partial t} + (u \cdot \nabla) T \right) = -\nabla \cdot (q_c + q_r) + \tau : S - \frac{T}{\rho} \frac{\partial \rho}{\partial T} \left[ \frac{\partial p}{\partial t} + (u \cdot \nabla) p \right] + Q \quad (2)$$

Where,  $\rho$  is the density ( $\text{kg/m}^3$ ),  $C_p$  is the specific heat capacity at constant pressure ( $\text{J}/(\text{kg} \cdot \text{K})$ ),  $T$  is absolute temperature (K),  $u$  is the velocity vector (m/s),  $q_c$  and  $q_r$  are the heat flux by conduction and radiation ( $\text{W/m}^2$ ),  $p$  is pressure (Pa),  $\tau$  is the viscous stress tensor (Pa),  $S$  is the strain-rate tensor ( $1/\text{s}$ ),  $Q$  contains heat sources other than viscous heating ( $\text{W/m}^3$ ). In order to treat radiation intensity equation numerically, the angular space is discretized and discrete ordinates method was implemented. Assuming that model is invariant in the  $z$  direction and discrete ordinates method in the form of radiative transfer equation in the direction of  $\Omega_{i+}$  and  $\Omega_{i-}$  expressed with the help of equation (3) and (4):

$$\Omega_{i+} \cdot \nabla I_{i+} = \kappa I_b(T) - \beta I_{i+} + \frac{\sigma_s}{4\pi} \sum_{j=1}^n \omega_j I_j \Phi(\Omega_j, \Omega_{i+}) \quad (3)$$

$$\Omega_{i-} \cdot \nabla I_{i-} = \kappa I_b(T) - \beta I_{i-} + \frac{\sigma_s}{4\pi} \sum_{j=1}^n \omega_j I_j \Phi(\Omega_j, \Omega_{i-}) \quad (4)$$

Computational conditions are given in Table 1 for this calculation.

Table 1. Computational condition

Incident radiation	250 W/m <sup>2</sup>
Wall types	Gray
Initial temperature	293.15 K
Outside Temperature	293.15 K
Reference pressure	1 atm
Method	Discrete Ordinate
Wall height	1600 mm

Computational grids were generated by using COMSOL software [8] and physics controlled mesh is used and extremely-coarse element size was chosen. Because no need to use high element size mesh for this calculation. Mesh distribution for solar pond is given in Figure 2.

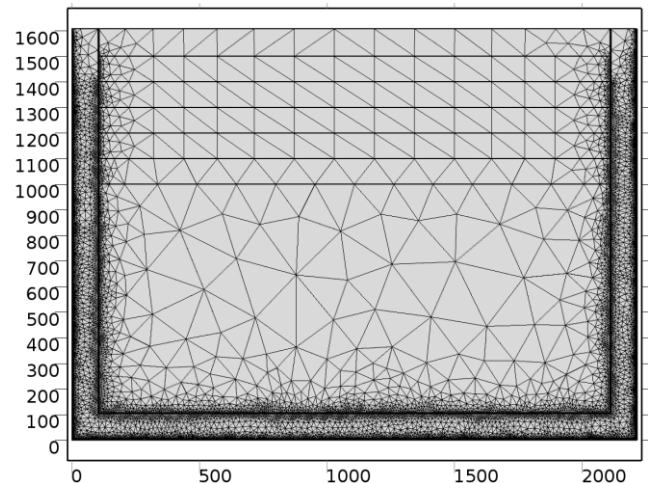


Figure 2. Mesh distribution for solar pond

### IV. RESULTS AND DISCUSSION

This study was conducted using COMSOL 4.3b simulation software for investigating temperature distribution of a solar pond. Numeric calculations were carried out for different insulation materials such as glass wool, foam and rock wool. The temperature distributions of the solar pond were calculated for different insulation materials and shown in Figure 3a-b-c. As seen in Figure 3, The temperature in the solar pond increases towards the bottom of the pond. The heat losses from the side walls and the surface of the pond cause the temperature decrease in this region. At the end of 720 hours, the temperature of HSZ was found to be reached 332 K.

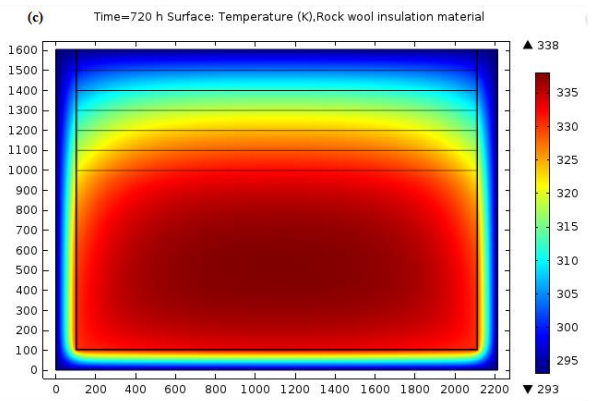
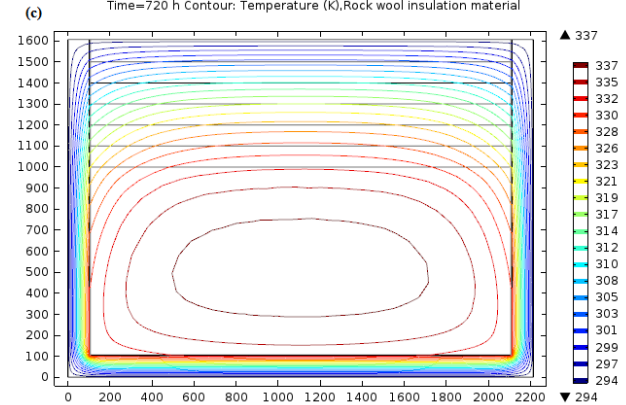
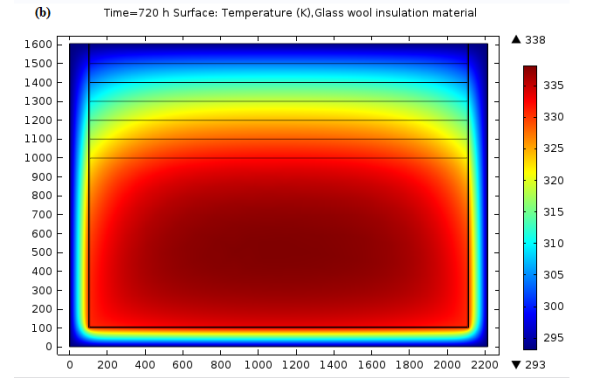
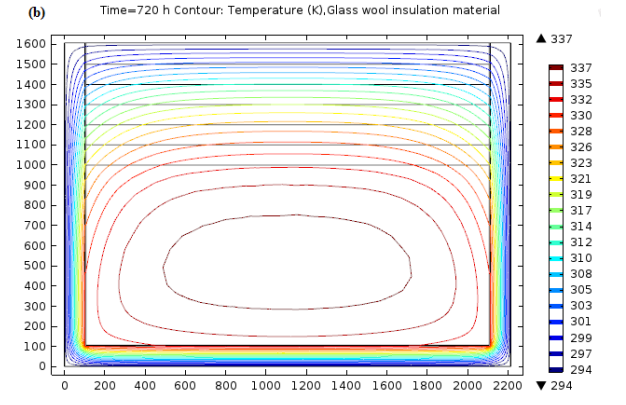
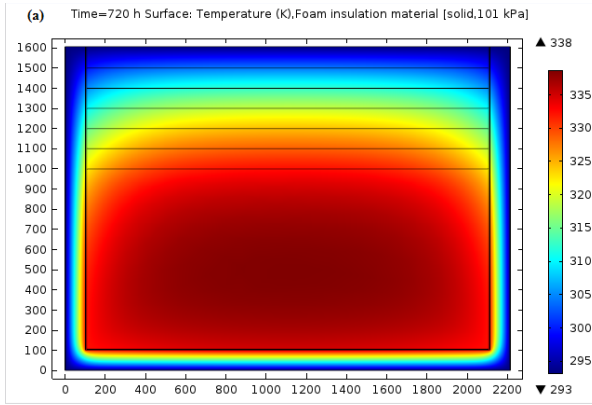
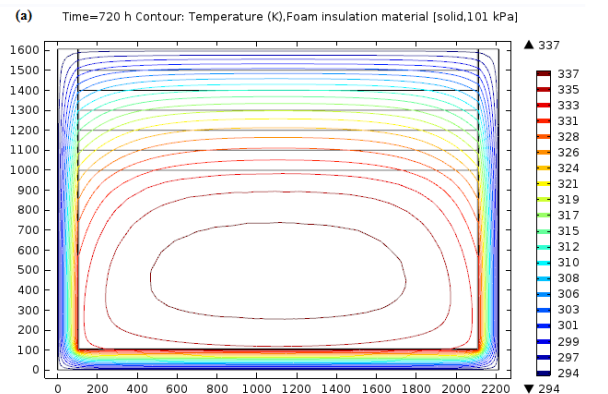
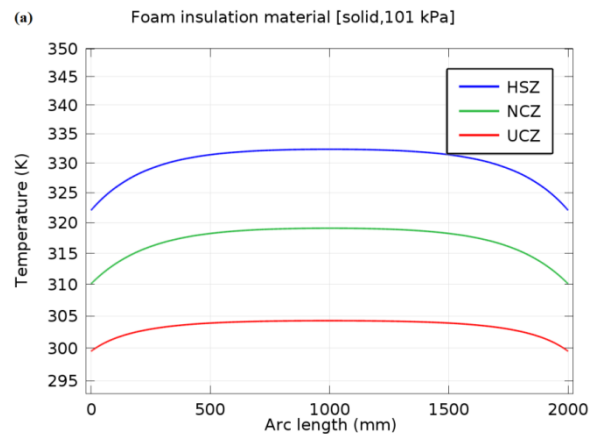


Figure 4. Isothermal contours distribution in the solar pond for a-foam, b-glass wool, c-rock wool

The temperature of the zones' line is shown in Figure 5 for different insulation materials. As seen in Figure 5, It is seen that the temperature decreases in parts close to the wall for all regions. This is due to the heat loss from the side walls.

Figure 3. Temperature distribution in the solar pond for a-foam, b-glass wool, c-rock wool

Figure 4 shows isothermal contours distribution in the solar pond for different insulation materials.



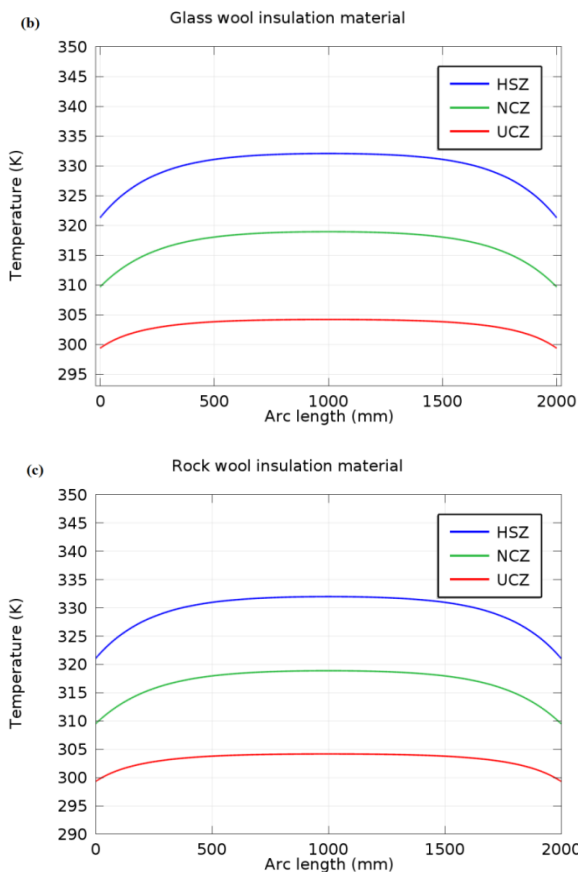
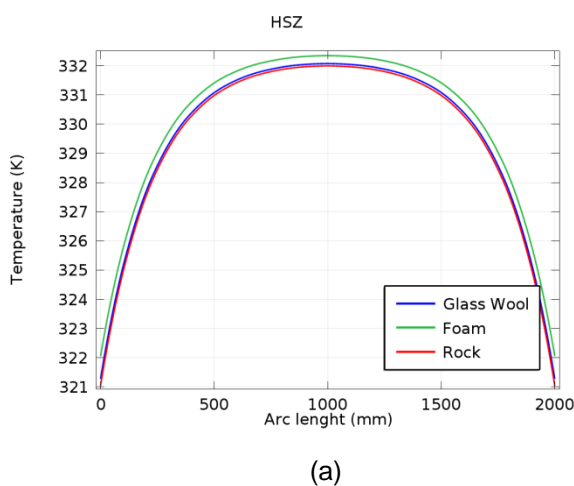
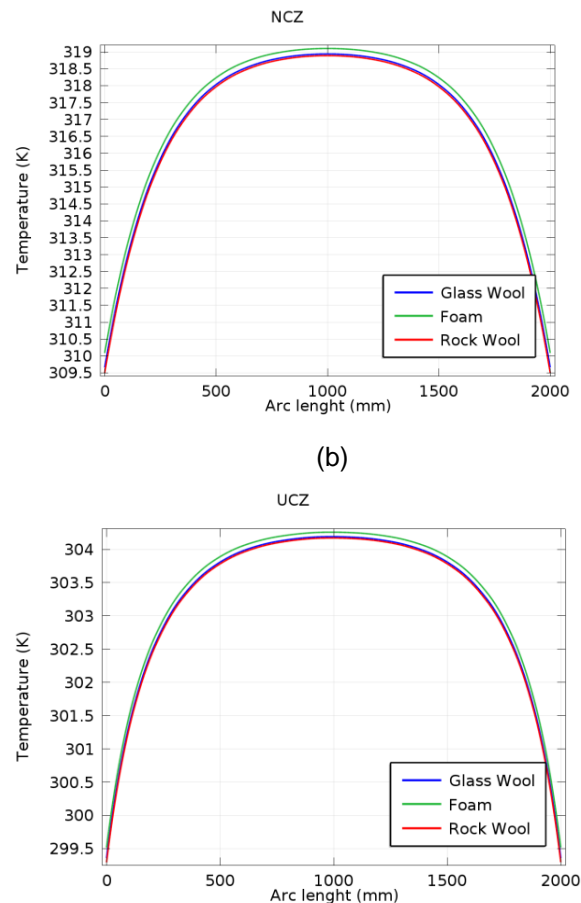


Figure 5. Temperature distribution in HSZ, NCZ and UCZ line

The temperature comparison of the zones for different used insulation materials is shown in Figure 6. As seen in Figure 6, when the foam is used as a insulation materials, maximum HSZ temperature is obtained. The temperature difference is low but if the system is run for a long time, it is clear that difference increases significantly.



(a)



(b)

(c)

Figure 6. The temperature comparison of the zones for different used insulation materials a-HSZ, b-NCZ, c-UCZ

## V. CONCLUSION

This paper numerically investigates temperature distribution of a solar pond for three different insulation materials. It is necessary to minimize heat loss for increasing the performance of solar pond. Heat losses can be reduced by making the side wall insulation very well. In the modeling, three different insulation materials were used in the same thickness. The temperature distribution of the inner zones were calculated and compared with different insulation materials. As a result, maximum temperature was obtained in the solar pond for using foam.

## ACKNOWLEDGMENT

I thank Middle East Technical University, allowing me to this work in there with their facility.

## NOMENCLATURE

HSZ	Heat storage zone
NCZ	Non-convective zone
UCZ	Upper convective zone
$\rho$	Density (kg/m <sup>3</sup> )

---

$C_p$	Specific heat capacity at constant pressure (J/kg·K)
$T$	Absolute temperature (K)
$u$	Velocity vector (m/s)
$q$	Heat flux by conduction (W/m <sup>2</sup> )
$p$	Pressure (Pa)
$\tau$	Viscous stress tensor (Pa)
$S$	Strain-rate tensor (1/s)
$Q$	Heat sources other than viscous heating (W/m <sup>3</sup> )
$U$	Internal energy (J)
$h$	Heat transfer coefficient (W/m <sup>2</sup> ·K).
$k$	Thermal conductivity of the fluid (W/m·K).
$q_0$	Inward heat flux (W/m <sup>2</sup> )

#### REFERENCES

- [1] L. Saylan, O. Sen, H. Toros, A. Arisoy, "Solar energy potential for heating and cooling systems in big cities of Turkey", *Energy Conversion and Management* 43, 2002, pp. 1829–1837.
- [2] M. Karakilcik, K. Kıymac, I. Dincer, "Experimental and theoretical temperature distributions in a solar pond", *International Journal of Heat and Mass Transfer* 49, 2006, pp. 825–835.
- [3] A. Sakhrieh, A. Al-Salaymeh, "Experimental and numerical investigations of salt gradient solar pond under Jordanian climate conditions", *Energy Conversion and Management* 65, 2013, pp. 725–728.
- [4] M. Karakilcik, I. Dincer, I. Bozkurt, A. Atiz, "Performance assessment of a solar pond with and without shading effect", *Energy Conversion and Management* 65, 2013, pp. 98–107.
- [5] M.M.O. Dahab, M. Ounib, A. Guizania, A. Belghith, "Study of temperature and salinity profiles development of solar pond in laboratory", *Desalination* 183, 2005, pp. 179–185.
- [6] I. Bozkurt and M. Karakilcik, "The effect of sunny area ratios on the thermal performance of solar ponds", *Energy Conversion and Management* 91, 2015, pp. 323–332.
- [7] I. Bozkurt and M. Karakilcik, "Exergy analysis of a solar pond integrated with solar collector", *Solar Energy* 112, 2015, pp. 282–289.
- [8] COMSOL CFD module user guide. <http://www.comsol.com>. 2015.